Available online at www.sciencedirect.com
ScienceDirect
International Journal of Heat and Mass Transfer 50 (2007) 433–443
International Journal of HEAT and MASS TRANSFER
www.elsevier.com/locate/ijhmt

A comparative evaluation of two different heat-recovery schemes as applied to a two-bed adsorption chiller

Xiaolin Wang, H.T. Chua *

School of Mechanical Engineering, The University of Western Australia, 35 Stirling Highway, WA 6009, Australia

Received 14 December 2005; received in revised form 2 August 2006
Available online 6 October 2006

Abstract

This study investigates the efficiency of two distinct heat-recovery schemes as applied to the two-bed silica gel–water adsorption chiller. Performance predictions stemming from an experimentally verified distributed-parameter model compare favorably with the experimental results at various operating conditions. Our study highlights the pivotal role played by heat-recovery schemes to ameliorate the chiller performance and substantially improve the coefficient of performance (or COP). The two different schemes essentially offer the same cooling capacity and similar COP boosting capability. In the studied working conditions of a two-bed adsorption chiller, the difference in COP by using the two schemes is less than 5%.

Keywords: Adsorption cooling; Silica gel; Heat-recovery; Chiller; Efficiency; Chiller performance

1. Introduction

Adsorption chillers have been commercialized for more than a decade. It has attracted a lot of attention from the scientific community and cooling industry due to its (i) utilization of waste heat for useful cooling; (ii) environmentally benign refrigerant and (iii) low maintenance cost. However, adsorption chillers have not been prevalently reduced to practice due to its low COP and high initial cost. How to improve the system performance is still a key issue for the fraternity.

Many operation schemes had been proposed to improve the chiller COP in the past 20 years. Douss et al. [1] and Wang [2] studied the performance of a cascading cycle in which activated carbon–methanol and zeolites–water were cascaded in the different beds. That cycle enjoyed a high COP; however, its sophistication presented an obstacle to commercialization. In a trial to improve the COP, Shelton and Wepfer [3] separately proposed a thermal wave cycle for an adsorption heat pump. Based on that work, Critoph [4] offered a forced convection regenerative cycle for the same purpose. Those two cycles were attractive but were difficult to apply in the field due to their low cooling throughput and costly adsorber design. Wang [5] subsequently investigated the combined effect of a continuous heat-recovery scheme and a mass recovery scheme. That scheme however, was predicated on the use of a high temperature heat source which precluded its use in silica gel–water adsorption chillers.

In the current market, only the water-circulation heat-recovery scheme is applied in commercial adsorption chillers by Nishiyodo Kuchouki Co. Ltd. [6] and Mayekawa Manufacturing Co. Ltd. [7]. In such a scheme during the bed switching period, the hot adsorber to be pre-cooled for adsorption transfers its heat to the cold desorber to be pre-heated for desorption. This configuration recovers the sensible heat stored in the heat exchanger matrix due to the thermal mass of materials and hence largely improves the system COP.

More recently, Wang et al. [8] proffered a passive heat-recovery scheme by delaying the water valve switching from the beginning of the switching period to a certain

* Corresponding author.
E-mail addresses: xlwang@mech.uwa.edu.au (X. Wang), htchua@mech.uwa.edu.au (H.T. Chua).

0017-9310/$ - see front matter © 2006 Elsevier Ltd. All rights reserved.
doi:10.1016/j.ijheatmasstransfer.2006.08.003

Nomenclature

c_p	specific heat capacity (J/kg K)
d	diameter (m)
D_s	surface diffusivity (m^2/s)
D_{so}	pre-exponent constant (m^2/s)
E_a	activation energy of surface diffusion (kJ/kg)
FS	fin spacing (m)
$\hbar$	heat transfer coefficient (W/m^2 K)
h	enthalpy (J/kg)
h_{fg}	latent heat of condensation or vaporization (J/kg)
k_D	permeability of porous media (m^2)
k	thermal conductivity (W/m K)
L	length (m)
m	mass (kg)
$\dot{m}$	mass flow rate (kg/s)
P	pressure (Pa)
q	fraction of refrigerant as adsorbed by the adsorbent (kg/kg dry adsorbent)
q^*	fraction of refrigerant which can be adsorbed by the adsorbent under saturation condition (kg/kg dry adsorbent)
r	radius (m)
t	time (s)
T	temperature (°C)
u	specific internal energy (J/kg)
v	velocity (m/s)
V	volume (m^3)
ΔH_{ads}	isostearic heat of adsorption (J/kg)
δ	fin thickness (m)
ε	porosity
μ	viscosity (N s/m^2)
ρ	density (kg/m^3)
τ	time constant (s)
COP	coefficient of performance

Superscripts/Subscripts

a-h	heat of adsorption
b	bed
c	condenser
chilled	chilled water
cond	condenser cooling water
cooling	cooling water
e	evaporator
f	fluid(water)
fin	fin
h	heat
heating	hot water
i	inner
in	inlet
l	liquid water, left
m	metal tube
mean	mean
o	outer
p	particle
p-h	pre-heating
p-c	pre-cooling
r	radial direction, right
rej	rejection
rev	recovery
s	silica gel
sorp	adsorption/desorption related to corresponding stage
t	total
v	water vapor
z	axial direction

stage of the normal operating period. Their experimental study confirmed that a passive heat-recovery scheme could substantially boost the system COP by a simple minor adjustment to the control logic and without having the need to introduce any additional hardware. Hence, it could be easily implemented in existing commercial adsorption chillers and possibly supplant the active water-circulation heat-recovery scheme at the design stage.

We shall show that by adopting the Nishiyodo water-circulation scheme, the details of which will be presented later, we are able to soundly explain some hitherto unexplained regenerative trends embedded in the chiller experimental data [9,10]. Specifically, we have achieved an excellent agreement between simulation and experiment particularly during the bed switching period when the hot-water outlet temperature actually approaches the hot-water inlet temperature. We shall then evaluate the efficiency of the Nishiyodo water-circulation scheme vis à vis our passive heat-recovery scheme and benchmark with actual experimental data [9,10] collected over assorted operating conditions.

2. The working principles of two heat-recovery schemes

Adsorption cycles encompass two processes: heating-desorption-condensation and evaporation-adsorption-cooling. The heating-desorption-condensation process requires energy input to pre-heat the cold bed and overcome the heat of desorption. The adsorption-cooling process enjoins the active dissipation of sensible heat and heat of adsorption. Fig. 1 shows the schematic of a two-bed adsorption chiller. In the conventional normal operation when bed 1 is cooled to sustain vapor adsorption, cooling water flows through bed 1 (acting as an adsorber) via valve V2 to dissipate the heat of adsorption. The bed is connected to the evaporator to boil the refrigerant.

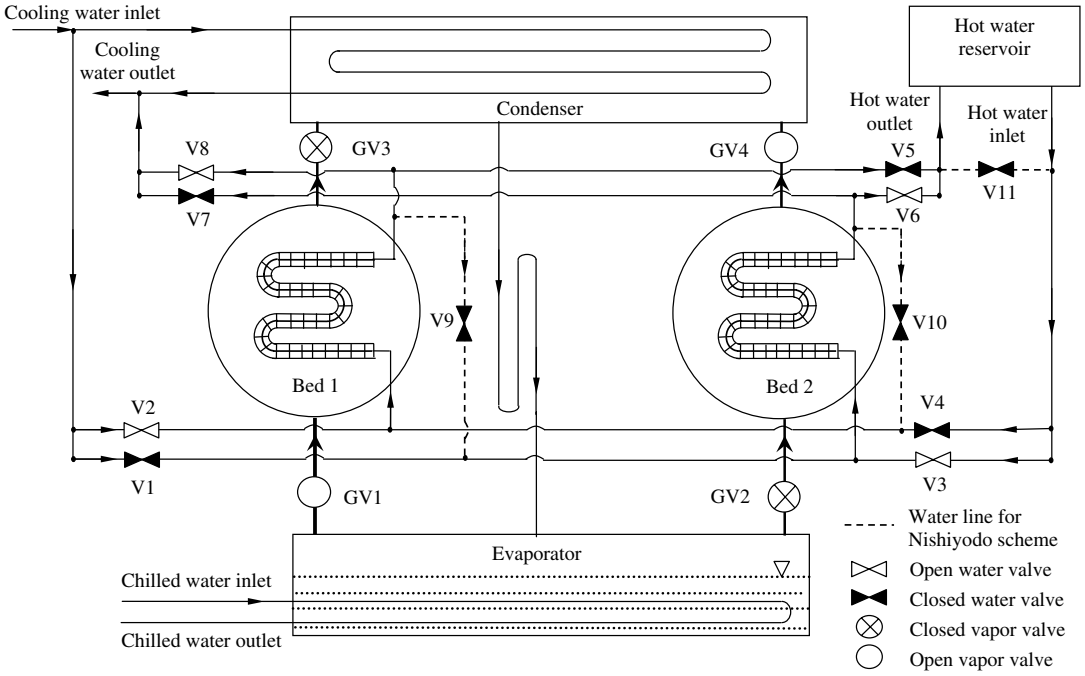

Fig. 1. A schematic of a two-bed silica gel adsorption chiller.

Meanwhile bed 2 is heated to maintain vapor desorption and the hot water flows through bed 2 (acting as a desorber) via valve V3 to provide the requisite energy. The bed is connected to the condenser to condense the refrigerant from the desorber. The operation phase is changed once the adsorber is nearly saturated and desorber purged of refrigerant. The ensuing transitional phase is called the switching process in which bed 1 is switched to a desorber and bed 2 to an adsorber. The desorber is cool due to its thermal mass and the residual cooling water in the heat exchanger and it must be pre-heated. The adsorber is hot due to its thermal mass and the remaining hot water in the heat exchanger. Hence, it must be pre-cooled. During the switching process, no refrigerant enters or leaves both the adsorber and the desorber. The total energy input Q_{input} to the chiller system includes the energy input Q_{h} during normal operation to promote desorption and sensible heat $Q_{\text{p-h}}$ during the switching process to pre-heat the desorber. The total energy rejection Q_{rej} comprises the heat of adsorption $Q_{\text{a-h}}$ generated during the adsorption process and sensible heat $Q_{\text{p-c}}$ for pre-cooling the adsorber during the switching process. In the standard operation scheme [9–11], the hot water and cooling water flow paths are changed at the same time as the beds are switched during the switching period. The hot water flows through the desorber (switched from an adsorber) en route to the hot-water reservoir and the cooling water meanders through the adsorber (switched from the desorber) on its way to the cooling tower. The sensible heat $Q_{\text{p-c}}$ is carried by the cooling water and rejected at the cooling tower. This precious energy is fully squandered. The extra energy equaling to $Q_{\text{p-h}}$ has to be externally provided by the hot water to pre-heat the desorber. It is imperative to note that the sensible heat $Q_{\text{p-c}}$ stems from not just the enthalpy of the entrapped hot water in the heat exchanger tubes of the desorber, but more substantially from the stored energy of the heat-and-mass transfer matrix in the desorber. The resultant COP is $Q_{\text{e}}/(Q_{\text{h}} + Q_{\text{p-h}})$.

The two heat-recovery schemes discussed herein essentially serve to recover the energy Q_{rev} from $Q_{\text{p-c}}$ to partially compensate for $Q_{\text{p-h}}$. The improved COP for a two-bed heat-recovery cycle is therefore $Q_{\text{e}}/(Q_{\text{h}} + Q_{\text{p-h}} - Q_{\text{rev}})$; the greater the Q_{rev}, the higher the COP. The Nishiyodo water-circulation scheme salvages the heat by transferring the energy inside the hot adsorber directly to the cold desorber. The cooling water flows into the hot adsorber and is heated by the energy stored therein. Subsequently the heated water flows into the cold desorber, partially imparts its energy to the desorber and then returns to the cooling tower. Meanwhile, the hot water bypasses the system to achieve energy saving. Hence, energy from the hot adsorber is used to pre-heat the cold desorber and thereby reducing the external energy input.

Our passive heat-recovery scheme [8] is markedly distinct from the Nishiyodo water-circulation scheme. It directly aims to reduce the energy drawn from the hot-water source instead of relying on an active energy transfer from the hot adsorber to cold desorber. During the switching period and in general a certain time period into the ensuing normal operating period, the switching of the system outlet valves is delayed to ensure that the high temperature water is always channeled back to the hot reservoir and the cold water pumped back to the cooling tower. The cooling water upon passing through the hot

adsorber is heated and directed to the hot-water reservoir instead of the cooling tower by delaying the switching of the valves 6 and 5 (i.e., V6 and V5, respectively in Fig. 1). Concomitantly, the hot water upon exchanging heat with the cold desorber is cooled and flows to the cooling tower by delaying the switching of valve 7 and valve 8 (i.e., V7 and V8, respectively in Fig. 1). This process lasts until the hot-water outlet temperature is equal to the cooling water outlet temperature. It is obvious that part of the sensible heat $Q_{p\text{-}c}$ is recovered and Q_{rev} is returned to the hot-water reservoir. Less energy will be required to heat the circulated hot water in the hot-water reservoir back to its pre-set temperature. Hence, the passive heat-recovery scheme attenuates the energy input to the chiller system and improves the COP.

Fig. 2 schematically compares the standard operation, passive heat-recovery and water-circulation heat-recovery schemes. The water flow paths in the various schemes are detailed in Table 1 in congruence with Fig. 1. The difference between the two heat-recovery schemes is salient. The Nishiyodo water-circulation scheme scavenges the heat by actively channeling energy from the hot adsorber to cold desorber. On the other hand, the passive heat-recovery scheme conserves energy by transferring energy from the hot adsorber to the hot-water reservoir so as to mitigate the external energy input. The passive heat-recovery scheme does not affect the adsorption/desorption process since the hot and cooling waters are only re-directed after emanating from the adsorber and desorber. The scenario is different in the Nishiyodo water-circulation scheme.

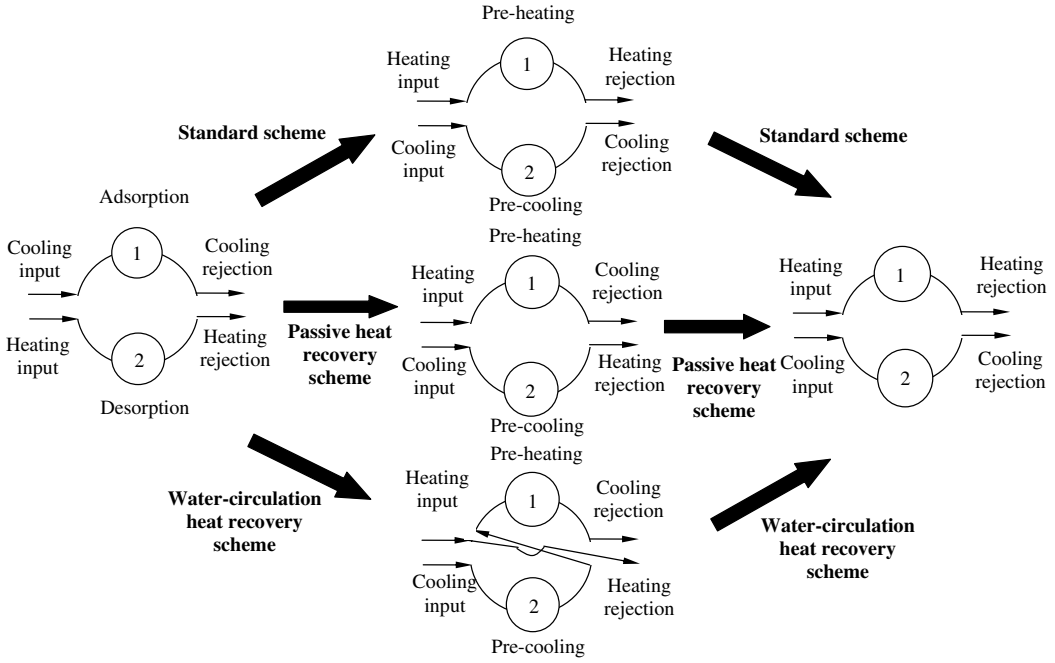

Fig. 2. A schematic of regenerative schemes with heating/cooling inputs/rejections.

Table 1
The water flow direction for different operating scheme

Stage	Beds' status		Water	Standard scheme	Valve scheme	Nishiyodo scheme
C1	Bed 1	A	Cooling	V2 → Bed 1 → V8	V2 → Bed 1 → V8	V2 → Bed 1 → V8
	Bed 2	D	Hot	V3 → Bed 2 → V6	V3 → Bed 2 → V6	V3 → Bed 2 → V6
SW	Bed 1	A–D	Hot	V4 → Bed 1 → V5	V4 → Bed 1 → V8	Hot water in →V11 → out
	Bed 2	D–A	Cooling	V1 → Bed 2 → V7	V1 → Bed 2 → V6	V1 → Bed 2 → V10 → Bed 1 → V8
C2	Bed 1	D	Hot	V4 → Bed 1 → V5	V4 → Bed 1 → V5	V4 → Bed 1 → V5
	Bed 2	A	Cooling	V1 → Bed 2 → V7	V1 → Bed 2 → V7	V1 → Bed 2 → V7
SW	Bed 1	D–A	Hot	V2 → Bed 1 → V8	V2 → Bed 1 → V5	Hot water in →V11 → out
	Bed 2	A–D	Cooling	V3 → Bed 2 → V6	V3 → Bed 2 → V7	V2 → Bed 1 → V9 → Bed 2 → V7
C1	Bed 1	A	Cooling	V2 → Bed 1 → V8	V2 → Bed 1 → V8	V2 → Bed 1 → V8
	Bed 2	D	Hot	V3 → Bed 2 → V6	V3 → Bed 2 → V6	V3 → Bed 2 → V6

A and D represents adsorption and desorption, respectively. C# means the normal operation time and SW represents switching period.

The cooling water heated by the hot adsorber serves to preheat the desorber. The temperature of this heated coolant is still lower than that from the hot-water reservoir. The resultant rate of desorber temperature increase is expectedly slower than that of the conventional and standard operation scheme. Hence, it may retard the desorption/adsorption process and somewhat reduce the cooling capacity at the same cycle time. In addition, the Nishiyodo water-circulation heat-recovery scheme requires three additional water valves and corresponding accessories such as piping works and modification of the control logic vis à vis the conventional and standard operation scheme. On the contrary, our passive heat-recovery scheme only mandates a modification to the control logic of those water valves at the system outlet. It dispenses with any additional hardware installation or modification and can be easily implemented in existing commercial chillers.

3. Mathematical modeling

The distributed-parameter model has been proven to exhibit a better agreement with the experimental data [12]. It is used herein to analyze the benefit of the two heat-recovery schemes since it employs the least empirical parameters in the simulation. The two-bed silica gel adsorption chiller analyzed was made by Nishiyodo Kuchouki Co. Ltd. The bed design incorporated a circular fin-tube heat exchanger. By using the control volume method, the modeling of mass and heat transfer inside the different components is summarized [12] below. One could consult Refs. [13,14] for a more detailed treatment of the transport phenomena in the beds.

3.1. Adsorber and desorber

The mass and energy balance for silica gel, tubes, fins and coolant inside the tubes can be written as

$$\int_V \varepsilon_t \frac{\partial \rho_v}{\partial t} + (1-\varepsilon_t)\rho_s \frac{\partial q}{\partial t}\,\mathrm{d}V = \begin{cases} \dot{m}_{e/c,v} & \text{normal operation} \\ 0 & \text{bed switching} \end{cases} \tag{1}$$

$$\frac{(1-\varepsilon_t)\partial\left(\rho_s c_{p,s} T_s + \rho_s(h_v - \Delta H_{ads})q\right) + \varepsilon_t \partial(\rho_v u_v)}{\partial t} = \frac{\partial\left(k_s \frac{\partial T_s}{\partial r} r\right)}{r\partial r} + \frac{\hbar_{fin,s}}{FS}(T_{fin,l} - T_s) - \frac{\hbar_{fin,s}}{FS}(T_s - T_{fin,r}) \tag{2}$$

$$\delta \frac{\left(\rho_{fin} c_{p,fin} T_{fin}\right)}{\partial t} = k_{fin}\delta \frac{\partial\left(\frac{\partial T_{fin}}{\partial r} r\right)}{r\partial r} + \hbar_{fin,s}(T_{s,l} - T_{fin}) - \hbar_{fin,s}(T_{fin} - T_{s,r}) \tag{3}$$

$$\rho_m c_{p,m} \frac{\partial T_{b,m}}{\partial t}\left(r_o^2 - r_i^2\right) = k_m \frac{\partial^2 T_{b,m}}{\partial z^2}\left(r_o^2 - r_i^2\right) + 2r_i \hbar_{f,m}(T_f - T_{b,m}) - 2r_o \hbar_{m,s}(T_{b,m} - T_s) + 2(1-\xi) r_o k_{fin} \frac{\partial T_{fin}}{\partial r} \tag{4}$$

and

$$\frac{\partial\left(\rho_f c_{p,f} T_f\right)}{\partial t} = -v_f \frac{\partial\left(\rho_f c_{p,f} T_f\right)}{\partial z} + \frac{\partial}{\partial z}\left(k_f \frac{\partial T_f}{\partial z}\right) - \frac{2\hbar_{f,m}}{r_i}(T_f - T_{b,m}) \tag{5}$$

The temperature boundary conditions are listed as

$$\text{Silica gel:}\quad -k_s \left.\frac{\partial T_s}{\partial r}\right|_{r=r_o} = \hbar_{m,s}(T_m - T_s); \qquad \left.\frac{\partial T_s}{\partial r}\right|_{r=r_{fin}} = 0 \tag{6}$$

$$\text{Metal tube:}\quad \left.\frac{\partial T_{b,m}}{\partial z}\right|_{z=0} = \left.\frac{\partial T_{b,m}}{\partial z}\right|_{z=L} = 0 \tag{7}$$

$$\text{Fins:}\quad T_{fin}|_{r=r_o} = T_m; \qquad \left.\frac{\partial T_{fin}}{\partial r}\right|_{r=r_{fin}} = 0 \tag{8}$$

$$\text{Coolant:}\quad T_f|_{z=0} = T_{cooling,in},\quad \text{when cooling;} \qquad T_f|_{z=0} = T_{hot,in},\quad \text{when heating;} \qquad \left.\frac{\partial T_f}{\partial z}\right|_{z=L_b} = 0$$

The pressure inside the adsorber is equal to the evaporator pressure and the pressure inside the desorber is equated to the condenser pressure. During the switching period, the pressure is determined from a mass-and-energy balance of the vapor inside the chamber and adsorbents by following a constant volume process. These mass and energy balance equations are as follows:

$$\frac{\mathrm{d}(\rho_{cham})}{\mathrm{d}t} = -\frac{1}{V_{cham}} \int_{V_h} \left[\varepsilon_t \frac{\partial \rho_v}{\partial t} + (1-\varepsilon_t)\rho_s \frac{\partial q}{\partial t}\right] \mathrm{d}V \tag{9}$$

$$\frac{\mathrm{d}(\rho_{cham} u_{cham})}{\mathrm{d}t} = -\frac{1}{V_{cham}} \int_{V_h} \left[\varepsilon_t \frac{\partial(\rho_v u_v)}{\partial t} + (1-\varepsilon_t)\rho_s h_g(T_s) \frac{\partial q}{\partial t}\right] \mathrm{d}V \tag{10}$$

In order to economize the computing time, the density change inside the porous volume is omitted since it is negligible in comparison to the adsorption/desorption term.

3.2. Condenser

The energy balance for the tubes and coolants are expressed as

$$\rho_m c_{p,m} \frac{\partial T_{c,m}}{\partial t} \frac{d_{c,o}^2 - d_{c,i}^2}{4} = k_m \frac{\partial^2 T_{c,m}}{\partial z^2} \frac{\left(d_{c,o}^2 - d_{c,i}^2\right)}{4} - d_{c,i}\hbar_{c,i}\left(T_{c,m} - T_{cooling}\right) + d_{c,o}\hbar_{c,o}(T_c - T_{c,m}) \tag{11}$$

and

$$\frac{\partial\left(\rho_f c_{p,f} T_{cooling}\right)}{\partial t} = -v_{cooling}\frac{\partial\left(\rho_f c_{p,f} T_{cooling}\right)}{\partial z} + \frac{\partial}{\partial z}\left(k_f \frac{\partial T_{cooling}}{\partial z}\right) - \frac{4\hbar_{c,i}}{d_{c,i}}\left(T_{cooling} - T_{c,m}\right) \quad (12)$$

The temperature boundary conditions are

$$\text{Tubes:}\quad \left.\frac{\partial T_{c,m}}{\partial z}\right|_{z=0} = 0; \qquad \left.\frac{\partial T_{c,m}}{\partial z}\right|_{z=L_c} = 0 \quad (13)$$

$$\text{Coolant:}\quad T_{cooling}\big|_{z=0} = T_{cooling,in}; \qquad \left.\frac{\partial T_{cooling}}{\partial z}\right|_{z=L_c} = 0 \quad (14)$$

3.3. Evaporator

The energy balance for the tubes and coolants are presented as

$$\rho_m c_{p,m}\frac{\partial T_{e,m}}{\partial t}\frac{\left(d_{e,o}^2 - d_{e,i}^2\right)}{4} = k_m \frac{\partial^2 T_{e,m}}{\partial z^2}\frac{\left(d_{e,o}^2 - d_{e,i}^2\right)}{4} + d_{e,i}\hbar_{e,i}\left(T_{chilled-T_{e,m}}\right) - d_{e,o}\hbar_{e,o}\left(T_{e,m} - T_e\right) \quad (15)$$

and

$$\frac{\partial\left(\rho_f c_{p,f} T_{chilled}\right)}{\partial t} = -v_{chilled}\frac{\partial\left(\rho_f c_{p,f} T_{chilled}\right)}{\partial z} + \frac{\partial}{\partial z}\left(k_f \frac{\partial T_{chilled}}{\partial z}\right) - \frac{4\hbar_{e,i}}{d_{e,i}}\left(T_{chilled} - T_{e,m}\right) \quad (16)$$

The mass and energy balance for the refrigerant is given as

$$\frac{dm_e}{dt} = \dot{m}_c - 2\pi\rho_s \int\int r\frac{dq}{dt}\,dr\,dz \quad (17)$$

and

$$\frac{\partial(m_e u_e)}{\partial t} = \dot{m}_c h_c - 2h_v\pi\rho_s \int\int r\frac{dq}{dt}\,dr\,dz + \int_0^{L_e} \hbar_{e,o}\pi d_{e,o}\left(T_{e,m} - T_e\right)dz \quad (18)$$

The temperature boundary conditions are

$$\text{Tubes:}\quad \left.\frac{\partial T_{e,m}}{\partial z}\right|_{z=0} = 0; \quad \left.\frac{\partial T_{e,m}}{\partial z}\right|_{z=L_e} = 0 \quad (19)$$

$$\text{Chilled water:}\quad T_{chilled}\big|_{z=0} = T_{chilled,in}; \qquad \left.\frac{\partial T_{chilled}}{\partial z}\right|_{z=L_e} = 0 \quad (20)$$

3.4. Adsorption equilibrium

The adsorption rate for the silica gel–water system is dictated by the linear driving force equation [15]. It can be expressed as

$$\frac{\partial q}{\partial t} = 15D_{s0}\exp\left(-E_a/RT_s\right)/R_p^2\cdot\left(q^* - q\right) \quad (21)$$

where q^* is the equilibrium vapor uptake at (T_s, P_s). The coefficients are obtained from the Fuji Davison Type A silica gel–water system and have been shown to be sufficiently robust to be applied to the present Fuji Davison Type RD silica gel–water system [12]. This equilibrium uptake is controlled by the following adsorption-equilibrium equation [16]:

$$q^* = \frac{K_0\exp\left\{\Delta H_{ads}/(R\cdot T)\right\}P}{\left[1 + \left\{K_0/q_m\cdot\exp\left(\Delta H_{ads}/(R\cdot T)\right)\cdot P\right\}^t\right]^{\frac{1}{t}}} \quad (22)$$

where q_m, K_0 and t are constants.

3.5. Performance equations

The cycle averaged cooling power, Q_{evap}, and COP are respectively defined as

$$Q_{evap} = \dot{m}_{chilled}\left[c_{p,f}\left(T_{chilled,mean}\right)\right] \times \int_0^{t_{cycle}}\left(T_{chilled,in} - T_{chilled,out}\right)dt \quad (23)$$

and

$$\text{COP} = \frac{Q_{evap}}{\dot{m}_{heating}\left[c_{p,f}\left(T_{heating,mean}\right)\right]\int_0^{t_{cycle}}\left(T_{heating,in} - T_{heating,out}\right)dt} \quad (24)$$

4. Result and discussion

The investigations described herein are conducted on a two-bed silica gel adsorption chiller made by Nishiyodo Kuchouki Co. Ltd. [10]. As we shall report below, we discover that the recently reported Nishiyodo water-circulation heat-recovery scheme [6] can aptly explain the assorted experimental data gathered from the chiller. We will also be comparing the simulation and experimental results at the various reported working conditions.

The water temperature at the outlets of the bed systems, condenser and evaporator is commonly used to characterize the adsorption/desorption behavior in adsorption cycles. Figs. 3 and 4 show the temperature histories at the outlets of the bed system, condenser and evaporator. The operation conditions are listed in Table 2. From the experimental results, it was evident that the hot-water outlet temperature returns back to the hot-water inlet temperature during the switching process. This hitherto enigmatic phenomenon consistently appeared in all the

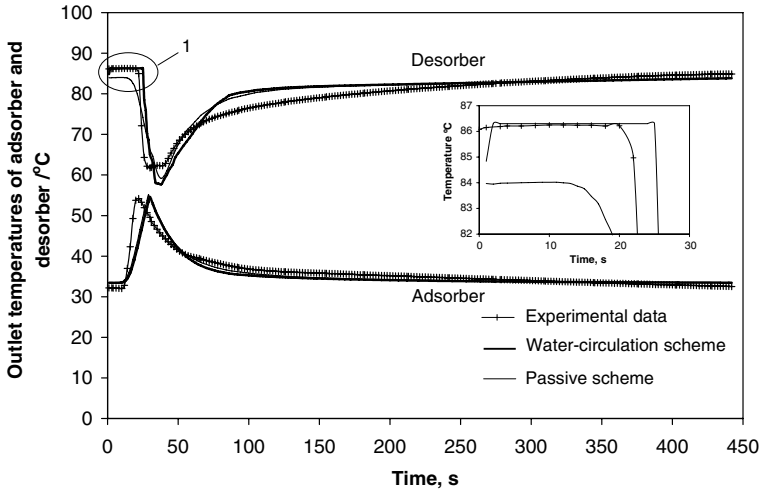

Fig. 3. A comparison of the system outlet temporal temperature profiles between the experiment and simulations.

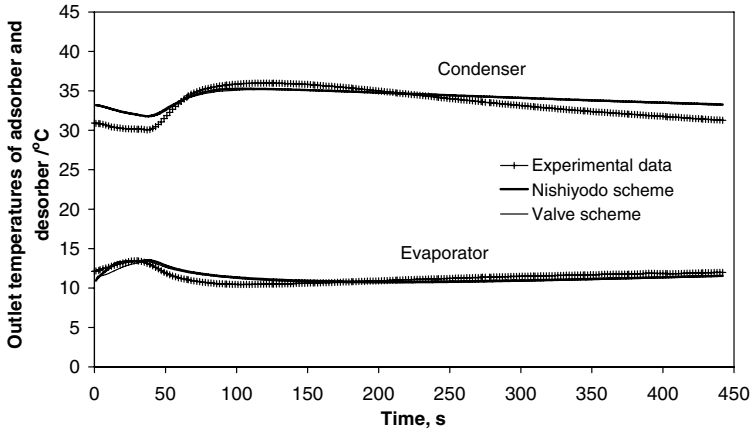

Fig. 4. A comparison of temperature histories at condenser and evaporator outlets between the experiment and simulations.

Table 2
Nominated operation conditions

Description	Temperature (°C)	Flow rate (kg/s)
Hot water to desorber	86.3	1.3
Cooling water to adsorber	31	1.6
Cooling water to condenser	31	1.3
Chilled water to evaporator	14.8	0.71
Cycle time (s)	442	
Switching time (s)	30	

working conditions reported in the literature [10]. None of the model reported heretofore succeeds in explaining this heat-recovery phenomenon [9,11,12]. This in turn implies that a water-circulation heat-recovery scheme was applied in this studied chiller. When we apply the Nishiyodo water-circulation scheme, the hot water bypasses the bed system during the switching period so that the temperature at the system inlet and outlet are the same. It is consistent with experimental findings. Furthermore, our simulation results exhibit a good agreement with the experimental results which further proves that the Nishiyodo water-circulation scheme has been applied in the chiller. The prediction results also accurately describe the experimentally observed precipitous drop in the hot-water outlet temperature and the sharp transition in the cooling water outlet temperature at about the end of the switching period which eluded all the previous simulation attempts [9,11,12]. In particular, as shown in the inset of Fig. 3, our simulation model incorporating the Nishiyodo water-circulation scheme fittingly explains why the hot-water outlet temperature regeneratively returns to the inlet temperature as the switching process progresses. Although our passive heat-recovery scheme and the associated simulation [8] can explain the temperature histories during the normal operation time, it fails to address the observed energy regeneration during the switching period as evidenced from the inset in Fig. 1. This further proves that the chiller was operated with the regenerative Nishiyodo water-circulation scheme. Regardless of the regenerative schemes used in our simulation, the time at which the hot-water temperature drops sharply is under predicted. This is because the valve

operating (on/off) time was not considered in the prediction model.

Fig. 5 demonstrates the efficiency of the two heat-recovery schemes. The corresponding working conditions are listed in Table 2. The area subtended between the hot-water inlet and outlet temperature curves represents the energy input for the system operation. The area covered between the chilled water inlet and outlet temperatures represents the cooling capacity. The ratio of chilled water area to hot-water area is essentially the system COP. The two schemes offer different hot-water outlet temperature profiles from the beginning of the switching process to the first part of normal operation stage. During the switching process, the hot-water outlet temperature in the water-circulation scheme is higher than that in the passive heat-recovery scheme as explained early and shown in Fig. 5. The former scheme recovers the energy more effectively than the passive heat-recovery scheme. However, the situation reverses in the first part of the normal operation scheme due to the retardation of the desorption process in the Nishiyodo water-circulation scheme. Therefore the areas covered by the hot-water inlet and outlet temperatures are almost the same for the two different processes. It was found that the two schemes substantially reduce energy input as indicated by the shading area in Fig. 5. In the abovementioned operation condition, the energy saving is around 40%. Thus the two schemes have almost the same COP boosting effect without compromising the cycle average cooling capacity. In the abovementioned working condition, the predicted cooling capacity by water-circulation heat-recovery scheme and passive heat-recovery scheme is respectively 10.3 kW and 10.7 kW and the COP is 0.36 and 0.37, respectively while the experimental cooling capacity and COP are 10.7 kW and 0.39, respectively.

Figs. 6 and 7 show the system performance map at different hot-water and chilled-water inlet temperatures. Table 3 delineates the corresponding experimental conditions. The results predicted by adopting the Nishiyodo water-circulation heat-recovery scheme exhibit a favorable agreement with the experimental data [10]. At the rated condition where $T_{\text{chilled}} = 14\ ^{\circ}\text{C}$, $T_{\text{hot}} = 85\ ^{\circ}\text{C}$, and $T_{\text{cooling}} = 30\ ^{\circ}\text{C}$, the simulation can accurately predict the COP and cooling capacity to within 9% and 2%, respectively. With decreasing chilled water temperatures, we over predict the experimental results for the cooling capacity and COP by up to 30% and 50%, respectively. Our kinetic

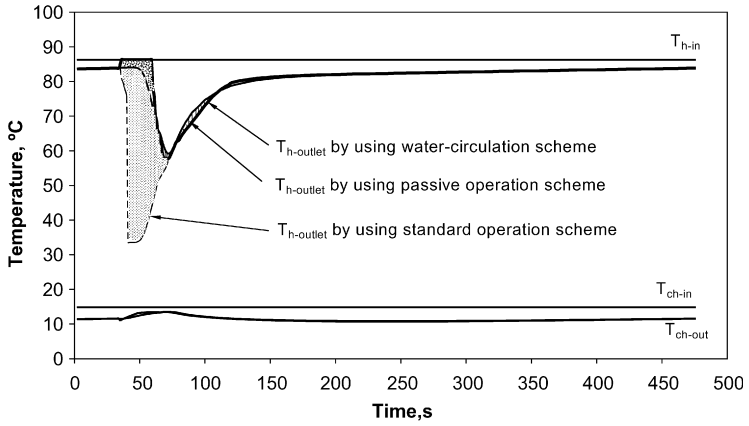

Fig. 5. A demonstration of energy saving by using the two heat-recovery schemes.

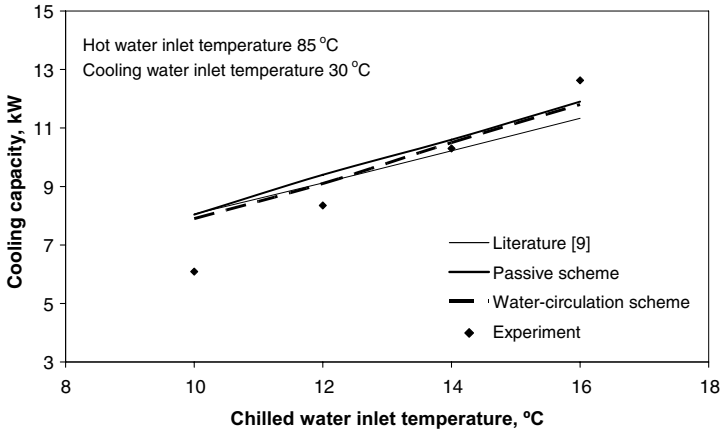

Fig. 6a. Cooling capacity predictions at 85 °C hot-water inlet temperature and 30 °C cooling water inlet temperature.

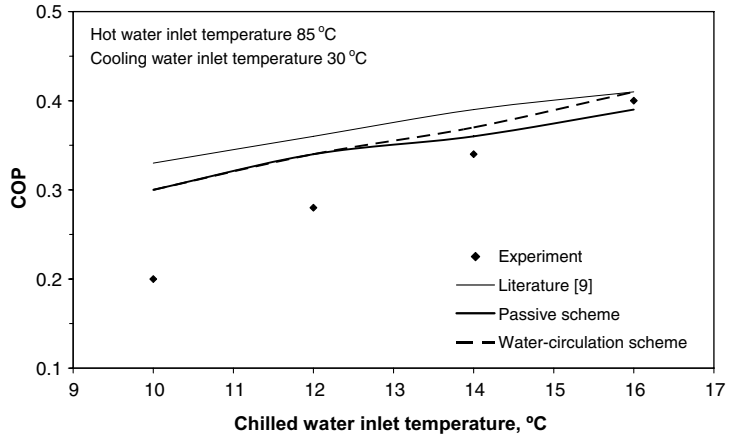

Fig. 6b. COP predictions at 85 °C hot-water temperature and 30 °C cooling water inlet temperature.

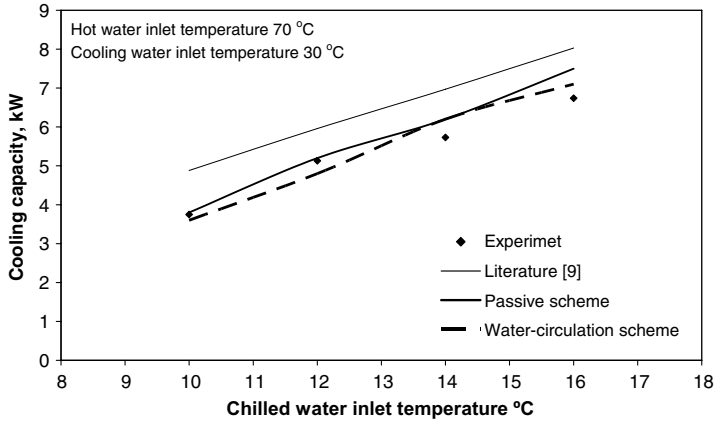

Fig. 7a. Cooling capacity predictions at 70 °C hot-water inlet temperature and 30 °C cooling water inlet temperature.

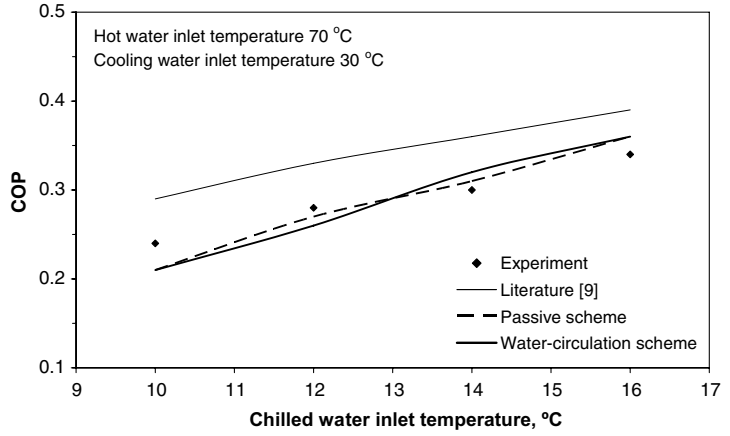

Fig. 7b. COP predictions at 70 °C hot-water temperature and 30 °C cooling water inlet temperature.

model for the adsorption of water vapor is ostensibly adequate to describe the boiling phenomenon at the evaporator under the rated conditions and therefore for chiller design. However, under substantially part-load conditions, the dearth of ebullient mass transfer data at low vacuum conditions give rise to a significant error in predicting the rate of mass transfer between the evaporator and the adsorber. We opine that this contributes to the major source of error in our simulation at part-loads and point to the need for more data accumulation to improve the chiller design model for part-load prediction. At $T_{hot} = 70\ ^{\circ}C$, our simulation also reliably predicts the

Table 3
Operation condition under different temperature

Description	Temperature (°C)	Flow rate (kg/s)
Hot water to desorber	85 and 70	1.3
Cooling water to adsorber	30	1.6
Cooling water to condenser	30	1.3
Chilled water to evaporator	10, 12, 14, 16	0.7
Cycle time (s)	450	
Switching time (s)	30	

Table 4
Operation condition under different temperature

Description	Temperature (°C)	Flow rate (kg/s)
Hot water to desorber	85	1.3
Cooling water to adsorber	31	1.6
Cooling water to condenser	31	1.3
Chilled water to evaporator	14	0.35
Cycle time (s)	120–780	
Switching time (s)	30	

system performance [10]. This demonstrates the robustness of the distributed-parameter modeling in relation to the commonly used lump-parameter models [9,11]. The passive heat-recovery scheme offers essentially the same trends and results as the Nishiyodo water-circulation scheme. This further proves that the two schemes effectively have the same efficiency of ameliorating the system performance.

Fig. 8 presents the effects of cycle time on COP and cycle average cooling capacity. The chiller operation conditions are listed in Table 4. A favorable agreement is obtained between experimental data [10] and simulation in which both show a peak in cooling capacity at around 400 s of cycle time and a tendency of the COP to increase with longer cycle time. However, with increasing cycle time, the distributed-parameter simulation over predicts the cooling capacity and COP at long cycle times. This is because the simulation assumes the same boiling heat transfer coefficient at all cycle times when in an actual situation the heat transfer efficiency is likely a function of cycle times. With longer cycle times, the adsorption driving force reduces and the intensity of boiling may reduce. Once again our passive heat-recovery scheme matches the Nishiyodo water-circulation scheme very well.

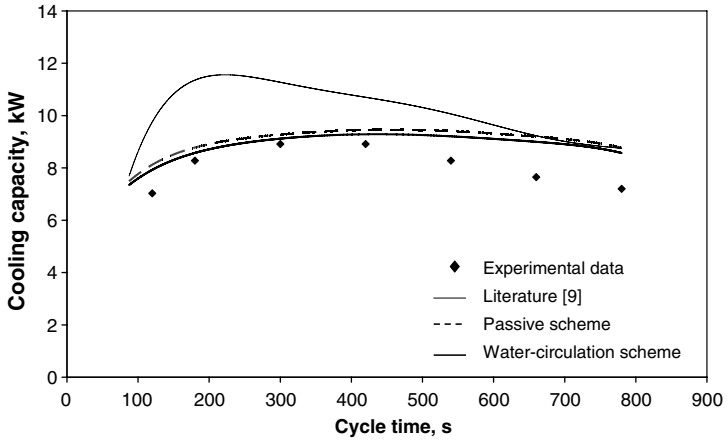

Fig. 8a. The effects of cycle time on cooling capacity.

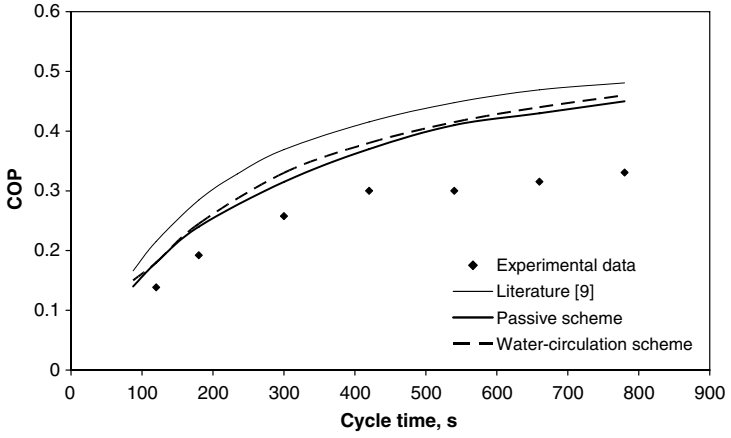

Fig. 8b. The effects of the cycle time on COP.

5. Conclusions

We have investigated the efficiency of two different heat-recovery schemes by using a verified distributed-parameter model at assorted operating conditions. Our predictions compare favorably with the corresponding experimental results. The recently reported Nishiyodo water-circulation heat-recovery scheme clearly clarifies the heretofore unexplained regenerative effect during the switching period in previously collected chiller data. Our recently reported passive heat-recovery scheme shows the same efficiency as the Nishiyodo water-circulation heat-recovery scheme. Both can substantially improve the system COP without affecting cycle average cooling capacity. The passive heat-recovery scheme can be easily adopted in the commercial chiller with a simple modification of system control logic and may be able to replace the Nishiyodo water-circulation heat-recovery scheme at the design stage.

Acknowledgement

We gratefully acknowledge BB Saha for making the chiller experimental data available to us.

References

[1] N. Douss, F.E. Meunier, L.M. Sun, Predictive model and experimental result for a two-bed adsorption air-conditioning, Ind. Eng. Chem. Res. 27 (2) (1998) 310–316.
[2] R.Z. Wang, Study on a four-bed cascade adsorption refrigeration cycle capable of COP over 1.1, in: Proc. of the 20th International Congress of Refrigeration, Sydney, September 1999, pp. 19–24.
[3] S.V. Shelton, W.J. Wepfer, Solid–vapor air conditioning technology, in: IEA Air conditioning Conference, Tokyo, 1990, pp. 525–535.
[4] R.E. Critoph, A forced convection regenerative cycle using the carbon–ammonia pair, in: Proc. of symposium: Solid Sorption Refrigeration, 1992, pp. 97–102.
[5] R.Z. Wang, Performance improvement of adsorption cooling by heat and mass recovery operation, Int. J. Refrig. 24 (2001) 602–611.
[6] HIJC USA, Inc. Waste heat adsorption chiller – function. Available from: <http://www.adsorptionchiller.bigstep.com/homepage.html>.
[7] Private communication with Mayekawa Manufacturing Company Ltd., 2003.
[8] X.L. Wang, H.T. Chua, K.C. Ng, Experimental investigation of silica gel–water adsorption chillers with and without a passive heat recovery scheme, Int. J. Refrig. 28 (5) (2005) 756–765.
[9] B.B. Saha, E.C. Boelman, T. Kashiwagi, Computer simulation of a silica gel–water adsorption refrigeration cycle – the influence of operating conditions on cooling output and COP, ASHRAE Trans. Res. 101 (2) (1995) 348–357.
[10] E.C. Boelman, B.B. Saha, T. Kashiwagi, Experimental investigation of a silica gel–water adsorption refrigeration cycle – the influence of operating conditions on cooling output and COP, ASHRAE Trans. Res. 101 (2) (1995) 358–366.
[11] H.T. Chua, K.C. Ng, A. Malek, T. Kashiwagi, A. Akisawa, B.B. Saha, Modeling the performance of two-bed silica gel–water adsorption chiller, Int. J. Refrig. 22 (1999) 194–204.
[12] H.T. Chua, K.C. Ng, W. Wang, C. Yap, X.L. Wang, Transient modeling of a two-bed silica gel–water adsorption chiller, Int. J. Heat Mass Transfer 47 (2004) 659–669.
[13] H.S. Al-Sharqawi, N. Lior, Conjugate computation of transient flow and heat and mass transfer between humid air and desiccant plates and channels, Numer. Heat Transfer, Part A: Appl. 46 (6) (2004) 525–548.
[14] M.N. Golubovic, W.M. Worek, Influence of elevated pressure on sorption in desiccant wheels, Numer. Heat Transfer, Part A: Appl. 45 (9) (2004) 869–886.
[15] A. Sakoda, M. Suzuki, Fundamental study on solar powered adsorption cooling system, J. Chem. Eng. (Japan) 17 (1) (1984) 52–57.
[16] J. Tóth, State equations of the solid–gas interface layers, Acta Chim. Acad. Sci. Hung. 69 (1971) 311–328.